Theoretical studies of Si and GaAs surfaces and initial steps in the oxidation

William A. Goddard III, John J. Barton, Antonio Redondo, and T. C. McGill

Arthur Amos Noyes Laboratory of Chemical Physics and Harry G. Steele Laboratory of Electrical Sciences, California Institute of Technology, Pasadena, California 91125

(Received 25 April 1978)

Using *ab initio* quantum chemical methods (generalized valence bond), we examine (i) the electronic states of Si (111) and GaAs (110) surface, (ii) the relaxation of the Si (111) surface, (iii) the reconstruction of the GaAs surface, (iv) the initial steps in the chemisorption of O_2 on Si (111), and (v) the bonding of O atom to Ga and As centers.

PACS numbers: 73.20.Cw, 82.65.−i

I. INTRODUCTION

The electronic properties of crystal surfaces play a crucial role in a number of important phenomena ranging from electrical properties of semiconductor devices to heterogeneous catalysts. There is presently little detailed understanding of the microscopic structure and properties of such surfaces but several new experimental and theoretical techniques are being applied to the study of the electronic properties of such surfaces. Our interest here will be in some of the theoretical approaches.

There are two quite different perspectives for thinking about surface states. One (which we refer to as the *band approach*) starts with an infinite solid and considers the disruption in the band states due to imposition of a surface. The other (which we refer to as the *chemical approach*) starts off with a finite molecule or complex representing the surface and considers the electronic states of this complex as the zero-order wavefunction. The modifications in these localized states due to extension of the finite molecule to the semiinfinite solid are then treated by gradually increasing the size of the complex. Carried to their limits, either description would lead to the same final answer; however, with a finite amount of effort, various aspects of the surface should be better treated with either the band or chemical approach.

A number of studies using band approaches[1] have been applied to the (111) surface of Si and the (110) surface of GaAs; however, there have been few studies using the chemical approach. Herein (Sec. III) we will use the chemical approach to study the (111) surface of Si and the initial species formed by bonding O_2 to the surface. In Sec. IV we will report similar calculations on the reconstruction of the (110) surface of GaAs and of the bonding of O atoms to Ga and As sites. In Sec. II we will outline the basic elements of the chemical approach, including some comparison with the band approaches.

Particular advantages in our approach are (i) Total energies are obtained; consequently, one can calculate directly the geometries of the reconstructed surface and of the chemisorbed species. (ii) Electron correlation (many-body) effects are included explicitly; in some cases the electron correlation effects are as large as several eV, while in other cases they are small, thus ignoring such effects can greatly distort the results.

The major disadvantage with the chemical approach is that the cluster sizes currently practicable are reather small. As a result, this approach may not provide an adequate description of the changes in the bulk band states due to the presence of the surface. In addition, it is currently quite difficult to handle sufficiently large clusters to study some rearrangements, e.g., the (7 × 7) reconstruction in Si (111).

II. THEORETICAL METHODS

Since the terminology for calculations using the band and chemical approaches is somewhat different, we provide in Sec. A.1 a brief review of simple Hartree–Fock theory, using notation common to the chemical approach. Section A.2 then provides an overview of the generalized valence bond method. Use of effective potentials for replacing core electrons is discussed in Sec. B.

A. Self-consistent field methods[2]

1. Hartree–Fock

A simple wavefunction for a many-electron system is the closed-shell wavefunction in which there are $N/2$ spatial orbitals, each occupied with one spin-up (α) electron and one spin-down (β) electron,[3]

$$\Psi^{CS}(r_1,r_2,\ldots,r_N) = \mathcal{A}\{(\phi_1\alpha)(\phi_1\beta)(\phi_2\alpha)(\phi_2\beta)\ldots\}, \quad (1)$$

where $\mathcal{A}$ is the antisymmetrizer or determinant operator and the spatial orbitals can be taken as orthonormal,

$$\langle\phi_i|\phi_j\rangle = \delta_{ij}. \quad (2)$$

The total energy of this wavefunction has the form

$$E = 2\sum_{i=1}^{N/2}(h_{ii} + J_{ii}) + \sum_{i>j=1}^{N/2} 2(2J_{ij} - K_{ij}) + \sum_{A>B}\frac{Z_A Z_B}{r_{AB}}, \quad (3)$$

where $h_{ii} = \langle\phi_i|h|\phi_i\rangle$ is the one-electron energy of orbital

 0022-5355/78/1504-1274$01.00

ϕ_i,

$$h(1) = -1/2\nabla_1^2 - \sum_A Z_A/r_{A1}$$

is the part of the Hamiltonian pertaining to a particular electron (1 in this case),

$$J_{ij} = \int d^3r_1\phi_i^*(1)\phi_i(1)\int d^3r_2 \frac{\phi_j^*(2)\phi_j(2)}{r_{12}} \tag{4}$$

is the Coulomb interaction between charge densities $|\phi_i|^2$ and $|\phi_j|^2$, and

$$K_{ij} = \int d^3r_1\phi_i^*(1)\phi_j(1)\int d^3r_2 \frac{\phi_j^*(2)\phi_i(2)}{r_{12}} \tag{5}$$

is the exchange interaction (involving orbitals of the same spin). Noting that

$$J_{ii} + K_{ii}, \tag{6}$$

Eq. (2) can be rewritten as

$$E = 2\sum_{i=1}^{N/2} h_{ii} + \sum_{i,j=1}^{N/2}(2J_{ij} - K_{ij}) + \sum_{A>B}\frac{Z_AZ_B}{r_{AB}} \tag{7}$$

The Hartree–Fock orbitals provide the lowest possible energy for Eq. (7), leading to the following variational equation (Euler–Lagrange equation),

$$H^{HF}\phi_i = \epsilon_i\phi_i \qquad (i = 1,2,\ldots,N/2) \tag{8a}$$

$$H^{HF} = h + \sum_{j=1}^{N/2}(2J_j - K_j), \tag{8b}$$

where $J_j(1)$ is the Coulomb potential at position r_1 due to charge density $|\phi_j|^2$,

$$J_j(1) = \int d^3r_2 \frac{\phi_j^*(2)\phi_j(2)}{r_{12}} \tag{9}$$

and K_j is the exchange operator defined so that

$$K_j\phi_i(1) = \phi_j(1)\int d^3r_2 \frac{\phi_j^*(2)\phi_i(2)}{r_{12}} \tag{10}$$

Within certain well-defined approximations (the Koopmans Theorem), each orbital energy, ϵ_i, in Eq. (8) (for occupied orbitals) corresponds to the negative of the ionization potential. Thus the ensemble of ϵ_i in Eq. (8) leads to a prediction of the photoemission spectrum (ignoring matrix element effects).

Note that a knowledge of the orbitals energies ϵ_i of Eq. (8) is *not* sufficient to determine the total energy. Thus from Eq. (8a)

$$\epsilon_i = h_{ii} + \sum_{j=1}^{N/2}(2J_{ij} - K_{ij}),$$

so that

$$2\sum_{i=1}^{N/2}\epsilon_i = 2\sum_{i=1}^{N/2}h_{ii} + 2\sum_{i,j=1}^{N/2}(2J_{ij} - K_{ij}). \tag{11}$$

Comparing with Eq. (7), we see that the two-electron energy is double-counted and the nuclear–nuclear repulsion energy is ignored.

For finite molecules, the H–F equations (8a) and (8b) are solved by expanding each MO, ϕ_i, in terms of a set of P atomiclike basis functions $\{\chi_\mu;\ \mu = 1,2\ldots,P\}$

$$\phi_i = \sum_{\mu=1}^{P}\chi_\mu C_{\mu i}, \tag{12}$$

converting the integro differential equations (8a) and (8b) to the form of (nonlinear) matrix equations

$$\sum_{\nu=1}^{P}(H_{\mu\nu}^{HF} - S_{\mu\nu}\epsilon_i)C_{\nu i} = 0, \tag{13a}$$

where

$$H_{\mu\nu}^{HF} = \langle\chi_\mu|H^{HF}|\chi_\nu\rangle \tag{13b}$$

and

$$S_{\mu\nu} = \langle\chi_\mu|\chi_\nu\rangle \tag{13c}$$

From numerous calculations it has been found that the smallest generally adequate basis set involves (on each nuclear center) (i) two basis functions for each atomic orbital of the atom (with the same angular character) and (ii) a full set of functions of angular momenta one higher than that of the valence orbitals. Thus for Ga one would include two sets of basis functions corresponding to 1*s*, 2*s*, 3*s*, and 4*s;* two sets corresponding to 2*p*, 3*p*, and 4*p;* two sets corresponding to 3*d* and one set corresponding to 4*d;* leading to a total of 41 basis functions. With use of effective potentials (vide infra) one need consider only the valence electrons and hence a set of 13 basis faunctions is quite adequate (the $n = 4$ functions above).

In order to carry out H–F calculations on solids, there are several types of approximations commonly made to Eq. (8) and (13).

(i) The Slater exchange approximation,[4]

$$\sum_j K_j \cong \alpha(81/4\pi)^{1/3}\rho^{1/3}, \tag{14}$$

where ρ is the charge density and $\alpha \sim 0.7$.

(ii) The muffin-tin approximation, where the total of all potential terms in H^{HF} is spherically averaged within some radius about each atom and taken as constant in the regions outside all spheres (but inside an outer sphere containing all inner spheres).[5]

(iii) Tight binding[6]: Only one basis function per valence atomic orbital is used, $S_{\mu\nu}$ is assumed orthonormal, and the matrix elements of Eq. (13b) are parameterized (for molecules this is referred to as extended Hückel theory[7]).

(iv) Pseudopotentials[8]: The core orbitals in Eq. (1) are ignored and their effect on Eq. (8) or (13) is mimicked by modifying h to include a pseudopotential whose terms are empirically adjusted to match experimental energy levels (vide infra).

With any of the above approximations, solution of the H–F equations, (8), leads to a set of orbital energies, ϵ_i, and hence to a predicted photoemission spectrum. However, with approximations (iii) and (iv) the one- and two-electron quantities are mixed together and it is not possible to extract the total energy. Consequently, one cannot solve directly for geometries. Although one can evaluate the total energy for the muffin-tin approximation, the resulting energies lead to ludicrous results (e.g., H_2O is linear[9]). Corrections to undo the

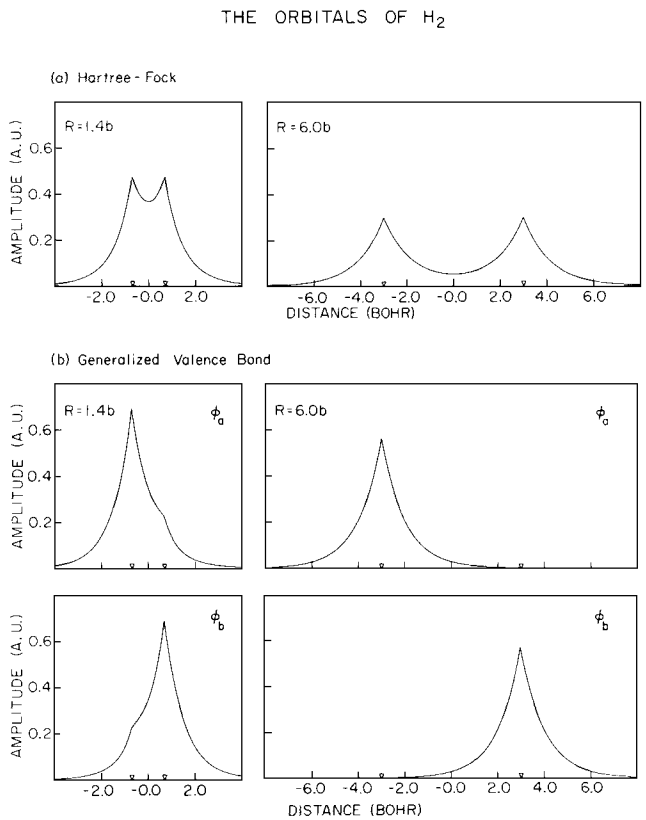

FIG. 1. The H–F and GVB orbitals for H_2. R is the internuclear distance; $R = 1.4\,b = 0.74$ Å is the equilibrium position.

muffin-tin approximation are possible; however, they are cumbersome and possible only for small systems.[10]

In order to study surface reconstruction and oxidation, it is necessary to calculate the total energy as a function of geometry. Essentially all band-type calculations include one of the above restrictions [(ii), (iii), or (iv)] preventing explicit evaluation of the total energy. Consequently we will turn to the chemical approach.

2. Generalized valence bond[2,11,12]

Even when carried out exactly, the Hartree–Fock wavefunctions are approximate wavefunctions of the system and are inadequate for some purposes. Particular difficulties with H–F theory are (i) the description of bond formation and dissociation and (ii) the relative location of low-lying excited states. As an example of (ii), H–F theory leads to a triplet lowest state of ozone (O_3), whereas the ground state is singlet with the triplet state 1 eV higher.[13] There are numerous examples of (i); we will consider the simplest case of H_2 in order to illustrate the origin of the problem and to compare various solutions.

The Hartree–Fock wavefunction for H_2 is[3]

$$a[\phi(1)\phi(2)\alpha(1)\beta(2)] = \phi(1)\phi(2)[\alpha\beta - \beta\alpha], \tag{15}$$

where

$$H^{HF}\phi = \epsilon\phi$$

and

$$H^{HF} = h + J_\phi. \tag{16}$$

By symmetry, ϕ is symmetric (gerade) and hence at large R (internuclear distance), ϕ has the form

$$\phi = \phi_l + \phi_r, \tag{17}$$

where ϕ_l and ϕ_r are localized on the left and right protons [see Fig. 1(a)]. Thus the spatial part of the two-electron wavefunction is[3]

$$\Phi^{HF} = \phi(1)\phi(2) = [\phi_l\phi_r + \phi_r\phi_l] + [\phi_l\phi_l + \phi_r\phi_r] \tag{18}$$

$$= \Phi_{cov} + \Phi_{ion} \tag{19}$$

At large R there is an equal amount of ionic and covalent character, whereas the exact wavefunction at $R = \infty$ is[3]

$$\psi^{exact}_{R=\infty} = (\phi_l\phi_r + \phi_r\phi_l)(\alpha\beta - \beta\alpha) \tag{20}$$

(where ϕ_l and ϕ_r are atomic orbitals). As a result, the H–F wavefunction leads to a terrible description at large R, as indicated in Fig. 2 (for H_2 the error at $R = \infty$ is 7.7 eV!). The problem is that in the H–F wavefunction the motions of the two electrons in ϕ are uncorrelated, resulting in too high a probability of being near each other. Generally, similar difficulties result for processes involving bond formation and bond disruption. Hence, to study chemisorption and the mechanism of oxidation we must include electron correlation or many-body effects.

An alternative form of H–F theory is the *unrestricted Hartree–Fock* (UH–F) wavefunction in which the up-spin and down-spin orbitals are allowed to be different and nonorthogonal,[3]

$$a[\phi_a(1)\phi_b(2)\alpha(1)\beta(2)] = \phi_a\phi_b\alpha\beta - \phi_b\phi_a\beta\alpha. \tag{21}$$

If ϕ_a and ϕ_b are different, this wavefunction describes a mixture of singlet and triplet, whereas $\phi_a = \phi_b$ leads to the closed-shell H–F wavefunction of Eq. (15). As shown in Fig. 2, the UH–F wavefunction is equivalent to the H–F wavefunction until $R = 2.6\,a_0 = 1.4$ Å. For larger R, the UH–F wavefunction goes continuously to the correct limit at $R = \infty$; however, at each R only about 25% of the bond energy is accounted for and hence the UH–F energy curve is not quantitatively useful.

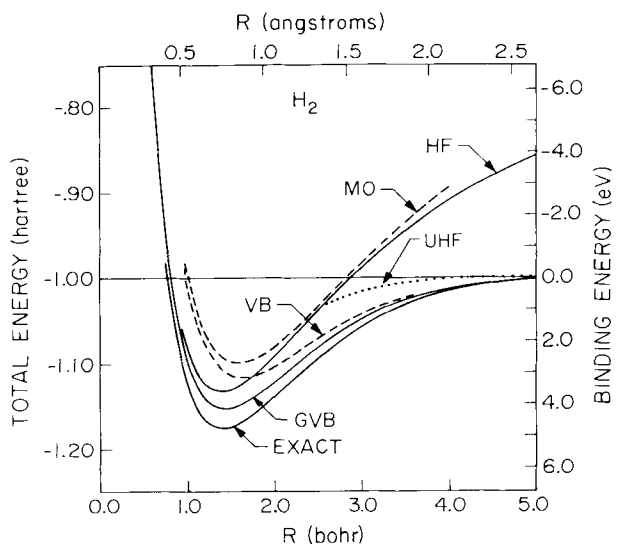

FIG. 2. The energy of H_2 as a function of internuclear distance for various wavefunctions.

An alternative approach, called the *valence bond* method, starts with the exace answer at $R = \infty$, (20), and uses the same form for finite R,[3]

$$\Psi^{VB} = (\phi_l\phi_r + \phi_r\phi_l)(\alpha\beta - \beta\alpha), \tag{22}$$

where ϕ_l and ϕ_r are 1s orbitals of H atom. Although exact for $R = \infty$ and qualitatively correct for smaller R, this wavefunction is not quantitatively useful for small R.

The *generalized valence bond* (GVB) wavefunction[11,12] uses one orbital per electron, as in VB, but solves self-consistently to obtain optimum orbitals as in HF. The resulting wavefunction has the form[3]

$$\Psi^{GVB} = (\phi_l\phi_r + \phi_r\phi_l)(\alpha\beta - \beta\alpha), \tag{23}$$

where the ϕ_l and ϕ_r resemble H atom orbitals that have polarized, contracted, and delocalized to some extend (see Fig. 1). For many-electron systems, it is convenient to transform each GVB pair [Eq. (23)] into (orthogonal) natural orbitals

$$\begin{aligned}\phi_g &= (\phi_l + \phi_r)/[2(1+S)]^{1/2} \\ \phi_u &= (\phi_l - \phi_r)/[2(1-S)]^{1/2}\end{aligned}, \tag{24}$$

where S is the overlap of the GVB orbitals.[2] With the GVB natural orbitals, Eq. (23) becomes

$$\Psi^{GVB} = [c_g\phi_g(1)\phi_g(2) - c_u\phi_u(1)\phi_u(2)]\alpha\beta - \beta\alpha), \tag{25}$$

where c_g and c_u are suitable coefficients. Comparing with the H–F wavefunction (15), we see that one natural orbital ϕ_g corresponds closely to the H–F orbital, while the other, ϕ_u, is responsible for the electron correlation effects. Thus the GVB wavefunction is the generalization of the H–F wavefunction in which electron correlation is incorporated and in which both the occupied and correlating orbitals are calculated self-consistently. The form of the variation equations for the GVB natural orbitals is[2]

$$H_g\phi_g = \epsilon_g\phi_g, \tag{26}$$

where

$$H_g = h - J_g - (c_u/c_g)K_u$$

and

$$H_u\phi_u = \epsilon_u\phi_u, \tag{27}$$

where

$$H_u = h + J_u - (c_g/c_u)K_g.$$

Note the close correspondence of Eq. (26) with (16). The form of Eq. (25) is easily generalized to allow more than two natural orbitals per electron pair (in order to include additional electron correlation effects). The detailed equations for GVB wavefunctions are reviewed elsewhere.[2]

After determining the self-consistent GVB orbitals, we generally carry out a configuration interaction calculation

$$\Psi^{CI} = \sum_i c_i\Psi_i \tag{28}$$

in which all configurations Ψ_i formed by various occupations of the GVB orbitals are allowed. This allows the inclusion of some additional electron correlation terms omitted in the GVB description and is most important at the saddle point for reactions. The resulting wavefunctions is referred to as GVB–CI.[14]

B. Core potentials

It has long been recognized that the core electrons (e.g., the He core of Li, the Ar core of Fe, the Ni core of Ge) do not change significantly upon binding various atoms together and that considerable computational simplicity could be obtained by replacing these core electrons with a pseudopotential[8,15] or effective potential.[16] In order to illustrate some of the important considerations we will discuss the case of Li atom.

The ground sate of Li has the configuration

$$(1s)^2(2s)$$

and wavefunction

$$\mathcal{A}[(\phi_{1s}\alpha)(\phi_{1s}\beta)(\phi_{2s}\alpha)], \tag{29}$$

where $\mathcal{A}$ is the antisymmetrizer or determinant operator. The (2s) orbital is an eigenfunction of the operator

$$H_v = h + (2J_{1s} - K_{1s}) \tag{30}$$

subject to the condition that the 2s orbital be orthogonal to the 1s orbital. Since $\mathcal{A}$ annihilates any component of 1s contained in the 2s orbital, we can mix in any amount of 1s character into the 2s orbital

$$\bar{\phi}_{2s} = (\phi_{2s} - \lambda\phi_{1s})/(1 + \lambda^2)^{1/2} \tag{31}$$

to obtain a new wavefunction

$$\mathcal{A}[(\phi_{1s}\alpha)(\phi_{1s}\beta)(\bar{\phi}_{2s}\alpha)], \tag{32}$$

whose properties are all identical to those of Eq. (29). Because the pseudo-orbital $\bar{\phi}_{2s}$ is not orthogonal to ϕ_{1s}, the operator $\bar{H}_v$ of which $\bar{\phi}_{2s}$ in Eq. (32) is an eigenfunction contains new (nonlocal) terms in addition to the terms contained in the H_v of Eq. (30), here we will just write $\bar{H}_v$ as

$$\bar{H}_v = h + \hat{V}_{1s}, \tag{33}$$

where $\hat{V}_{1s}$ contains all the terms involving the 1s orbital.

Although all properties of Eq. (32) are identical to all properties of Eq. (29), the expression used to evaluate these properties may be much different. For example, from Eq. (29) the charge density is

$$\rho = 2\phi_{1s}^2 + \phi_{2s}^2, \tag{34}$$

whereas from Eq. (32) it is

$$\rho = [2\phi_{1s}^2 + \bar{\phi}_{2s}^2 - 2S\phi_{1s}\bar{\phi}_{2s}]/(1 - S^2), \tag{35}$$

where

$$S = -\lambda/(1 + \lambda^2)^{1/2} \tag{36}$$

is the overlap between ϕ_{1s} and $\phi_{\bar{2}s}$. Although the densities derived from Eqs. (34) and (35) are identical, the way in which ρ is evaluated for the pseudo-orbital $\bar{\phi}_{2s}$ is much different from the evaluation of the usual orthogonal orbital ϕ_{2s}. Rewriting Eq. (35) as

$$\rho = 2\phi_{1s}^2 + \bar{\phi}_{2s}^2 + \Delta\rho,$$

the correction term $\Delta\rho$ is

$$\Delta\rho = [S^2(2\phi_{1s}^2 + \bar{\phi}_{2s}^2) - 2S\phi_{1s}\bar{\phi}_{2s}]/(1 - S^2). \quad (37)$$

This quantity $\Delta\rho$ is the error that would be made if, in using the pseudo-orbital $\bar{\phi}_{2s}$, the density were calculated using the simple expression (34).

1. Pseudopotentials

A common approach[8,15] to core potentials is to replace $\hat{V}_{1s}$ in Eq. (33) with an empirical potential V_p chosen so that the spectrum of eigenvalues from

$$h + V_p \quad (38)$$

matches the experimental spectrum of the atom or the band spectrum of the solid.[17,18] We will refer to this as the pseudopotential approach. Usually V_p is chosen so that the lowest orbital ($\bar{\phi}_{2s}$) is smooth, thereby making an explicit choice for the overlap with the core orbitals [λ in Eq. (31)]. This approach has been invaluable in elucidating the band spectrum of solids[17,18] but it has several deficiencies which we believe limit its usefulness for studies of surfaces.

(1) Choosing V_p to obtain the correct eigenvalue spectrum does *not* ensure that the *shapes* and *sizes* of the pseudo-orbitals will be correct. Consequently, the interaction of valence orbitals on different atoms could be quite wrong, leading to incorrect bond lengths and hybridization effects. If V_p is obtained by fitting the band spectrum of the solid and if V_p is only used for obtaining the band spectra of infinite solids, this may not be a significant problem. However, use of such a V_p for a surface could lead to a bad description of the hybridization and size of the surface orbitals.

(2) Using the V_p one can obtain the one-particle eigenvalues (i.e., orbital energies or band spectrum) of the system; however, there is no direct way to abstract the total energy as required in order to solve for geometries. This is particularly unfortunate since geometries of reconstructed surfaces and chemisorbed molecules would be quite valuable.

(3) Although the pseudopotentials can be made rigorous for the atom [as in Eqs. (31)–(37)], there are problems with their use in molecules. Even ignoring the problem in item 2, a nonzero λ in Eq. (31) leads to a valence orbital which is reduced in size by $(1 + \lambda^2)^{1/2}$ at large R. Thus the Coulomb and exchange interactions between valence orbitals on different atoms are modified.

(4) Even for the atom there are difficulties in the usual pseudopotentials if the atom has more than one valence electron. For example, the valence–valence interaction energy of the ground state of Ga is

$$J_{4s,4s} + 2J_{4s,4p} - K_{4s,4p}. \quad (39)$$

Replacing the Hartree–Fock 4*s* and 4*p* orbitals with pseudo-orbitals [as in Eq. (31)] containing core character [1*s*,2*s*,3*s*,2*p*,3*p*] leads to orbitals $\overline{4s}$ and $\overline{4p}$ which will, in general, have quite different values for $J_{\overline{4s},4s}$, $J_{\overline{4s},\overline{4p}}$, and $K_{\overline{4s},\overline{4p}}$. As a result, the use of pseudopotentials leads to some implicit modification in the values for the valence–valence interaction energies. This may change excitation energies, bond energies, and geometries.

(5) Often pseudopotential calculations make use of the Poisson equation,

$$\nabla^2 V = \rho \quad (40)$$

to relate charge density ρ to electrostatic potential V, but without including the correction term $\Delta\rho$ [see Eq. (37)].[15,17,18] This introduces additional approximations.

(6) After calculating the pseudopotentials, one would like to examine the charge distribution near the surface to learn about special effects arising from termination of the lattice. Again, because of the correction term $\Delta\rho$, these need not be physically significant.[19]

To some extent the problems in items (3), (4), and (5) are reduced for bulk band spectra by fitting the pseudopotential empirically to obtain the correct spectrum. However, this does not assure that these errors will be minor when treating a system as different as that of a surface. On the other hand, items (2) and (6) are intrinsic. There is no direct way to get total energies from pseudopotential calculations and the charge densities and other properties from pseudo-orbitals need not be physically significant [unless corrections of the type in Eq. (37) are included].

A suggestion has been made that potential curves be calculated by using the Hellmann–Feynman theorem to relate forces on the atoms to charge densities.[20] This has two difficulties: First, the Hellmann–Feynman theorem relates to the total density and not to the pseudodensity, and hence this approach is invalidated by the problem in item (6). Second, even very accurate wavefunctions from rigorous *ab initio* calculations can lead to large errors in the Hellmann–Feynman theorem[21] (that is, a wavefunction of sufficient quality to yield accurate geometries may have large Hellmann–Feynman forces at R_e). Consequently, this approach could lead to questionable results (e.g., it was recently shown[22] that use of this method can lead to a stronger bond of an H atom to tetrahedrally bonded Si than to a divalent Si).

2. Ab initio effective potentials

In our calculations we have used effective potentials[16,23] to replace the core electrons of Si, Ga, and As. The valence electrons are treated explicitly so that only the Ne core

$$(1s)^2(2s)^2(2p)^6 \quad (41)$$

of Si and the Ni core

$$(1s)^2(2s)^2(2p)^6(3s)^2(3p)^6(3d)^{10} \quad (42)$$

of Ga and As are replaced by effective potentials. The approach used here is to first carry out all electron *ab initio* calculations for several states of the atom and then to find a core potential that leads to the same energies and shapes for the valence orbitals.

We will illustrate the procedure for As. We solved (all-electron) for the high-spin states of the

$$[\mathrm{Ni}](4s)^2(4p)^3 \quad (43)$$

$$[\mathrm{Ni}](4s)^2(4p)^2(4d) \quad (44)$$

$$[\mathrm{Ni}](4s)^2(4p)^2(4f) \quad (45)$$

configurations of As where [Ni] is given in Eq. (42). The core

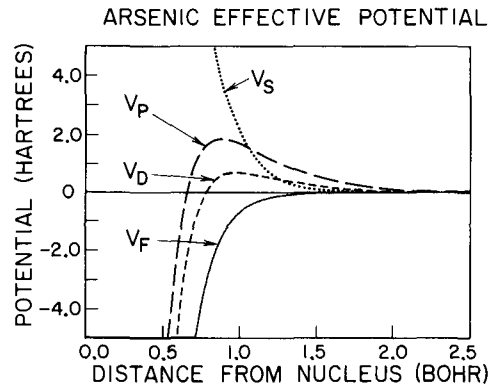

FIG. 3. The *ab initio* core effective potentials for As.

potential was taken to be of the form

$$\hat{V}_{As} = V_{sf}\hat{P}_s + V_{pf}\hat{P}_p + V_{df}\hat{P}_d + V_f,$$

where V_{sf}, V_{pf}, V_{df}, and V_f are local functions of r (distance from the As nucleus) and $\hat{P}_l$ is an angular momentum projection operator, projecting onto all components of angular momentum l. Previous studies[16] have shown that the core potentials for angular momenta represented in the core are very different from the higher angular momenta (because of the Pauli orthogonality condition), requiring such nonlocal terms.

For s, p, and d states of the atom, the total potentials operating on orbitals of the appropriate symmetry are

$$\begin{aligned} V_s &= V_{sf} + V_f \\ V_p &= V_{pf} + V_f \\ V_d &= V_{df} + V_f, \end{aligned} \tag{46}$$

while for all higher angular momenta the potential is V_f. These potentials are shown in Fig. 3.

As indicated above, the valence $4s$, $4p$, and $4d$ orbitals are nonunique and the core character in these orbitals was chosen so that (i) the valence–valence interactions are unchanged and (ii) the long-range amplitude of the orbital is unchanged. With these conditions, a least-squares procedure was used to obtain V_{sf}, V_{pf}, V_{df}, and V_f so that the solution of the new five electron problem using $\hat{V}_{As}$ reproduces the *ab initio* orbitals and energies.

Calculations on molecular systems use this *ab initio* effective potential V_{As} with no further readjustments. Since the shapes and sizes of the orbitals are correctly described, we expect both bond lengths and bond angles to be accurately predicted. This approach to *ab initio* core effective potentials eliminates difficulties (1), (2), (3), and (4) of pseudopotentials, while difficulty (5) is not relevant for our calculations. For charge densities there is a correction term analogous to Eq. (37); however, this correction term is zero outside of the core region. In this paper we will quote densities in terms of atomic populations so that no ambiguity results.

III. Si CALCULATIONS

A. Relaxation

The unreconstructed (111) surface of Si is illustrated in Fig. 4. In modelling this surface we consider that a finite portion

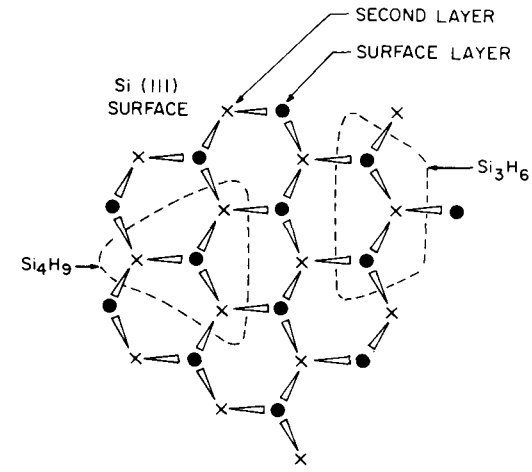

FIG. 4. The top two layers of the Si (111) surface.

of the surface is sliced out of the solid and every Si–Si bond so cut is replaced by a bond to an H atom.[24,25] In this way the proper hybridization is retained at each atom and there are no extraneous radical centers. Thus for modelling the relaxation of a surface Si atom we use the Si_4H_9 cluster obtained by selecting the surface Si, its three Si neighbors, and nine H's to replace the other bonds to the latter Si atoms.

The resulting dangling bond orbital is shown in Fig. 5. It is basically a Si $2p$ orbital (90% p character) mainly localized (90%) on the surface Si atom. Even so, important asymmetries arise from the presence of the bulk atoms. For example, the fact that the surface orbital is orthogonal (Pauli principle) to the bond between the second- and third-layer atoms causes a nodal plane in this region (see Fig. 5) and results in a moderate secondary amplitude in the third-layer atom. This orbital asymmetry may be responsible for the asymmetry detected in the angular-resolved photoemission from the surface orbitals.[26]

The total distance from the surface layer of Si atoms to the second layer is 0.79 Å; we find that the surface Si layer relaxes by 0.08 Å toward the bulk.[24] This same effect occurs in iso-

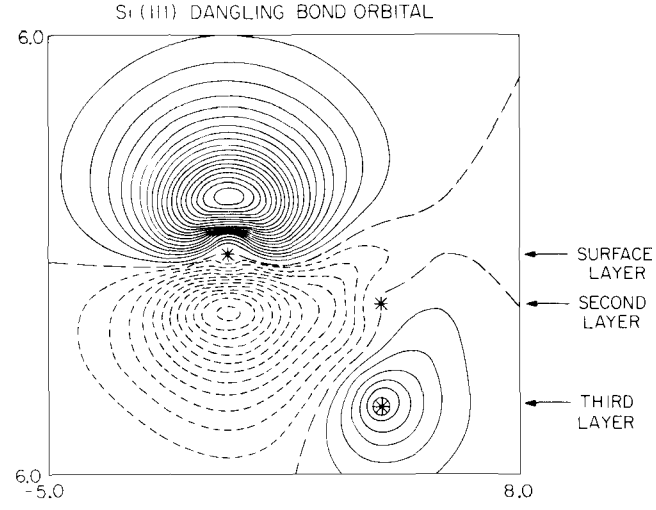

FIG. 5. The Si (111) dangling bond orbital. From calculations on Si $(SiH_3)_3$ with 0.08 Å relaxation. The long dashed line indicates the nodal plane. Solid lines indicate positive amplitude while short dashed lines indicate negative amplitude. The increment in contour lines is 0.01 atomic units.

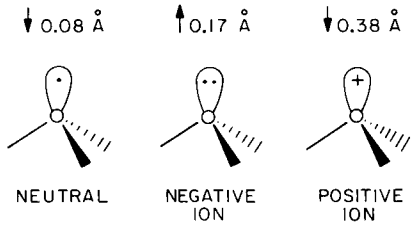

FIG. 6. The calculated relaxation distortions of the surface Si for the (111) surface. From calculations on the Si $(SiH_3)_3$ complex. The separation of the top two layers is 0.79 Å.

lated SiH_3, where the molecule is pyramidal but with bond angles larger than tetrahedral. Recently (after publication of the calculations) an experimental value for the surface layer relaxation of 0.12 ± 0.04 Å has been obtained from LEED dynamic intensity studies (the surface 1 × 1 surface was stabilized by submonolayers of Te).[27]

On the other hand, removing the electron from the dangling bond orbital leads to a large contraction of 0.38 Å (toward the bulk), 50% of the original interlayer spacing. Similarly, free SiH_3^+ is expected to be planar (or nearly so).

Placing an extra electron in the dangling bond orbital leads to distortion of the surface Si away from the bulk by 0.17 Å. This is consistent with expectations since the free SiH_3^- species would have HSiH bond angles close to 93°. The magnitudes of these distortions are indicated in Fig. 6.

We have not examined the 2 × 1 and 7 × 7 reconstruction of Si; however, recent experimental results[28] indicate that these reconstructions may involve only small modulations on a surface in which the average displacement of the surface Si is about 0.08 Å (toward the bulk).

B. Oxidation

1. The electronic states of O and O_2

In order to understand the initial steps in the oxidation of Si, it is appropriate to review the character of O atom and O_2 molecule.

The ground state of O atom has the configuration

$$(1s)^2(2s)^2(2p)^4$$

but the (1*s*) and (2*s*) orbitals can be ignored in the qualitative consideration. With three *p* orbitals for four electrons, the ground state (triplet) of O has one *p* orbital doubly-occupied and the other two singly occupied. This is illustrated by the orbital diagram Eq. (47), where 8 and ∞ indicate *p* orbitals

(47)

in the plane, ◯ indicates a *p* orbital out of the plane, and the dots indicate the number of electrons. The excited singlet state of O atom (2 eV excitation energy) is formed from configurations like Symbol (47) plus configurations of the form

(48)

with two doubly occuped *p* orbitals.

The ground state of O_2 is formed by pairing together ground state O atoms, configuration (47), so as to form a bond between singly occupied *p* orbitals where in each case there are two dominant (resonant) configurations.[12,29] Configuration (49) leads to the ground state of O_2, with the two singly occupied orbitals paired to a triplet state (*S* = 1). Configuration (50) leads to the excited singlet states of O_2 ($^1\Delta_g$ at 1.0 eV and $^1\Sigma_g^+$ at 1.6 eV) and the singlet combination of (49) also leads to $^1\Delta_g$.

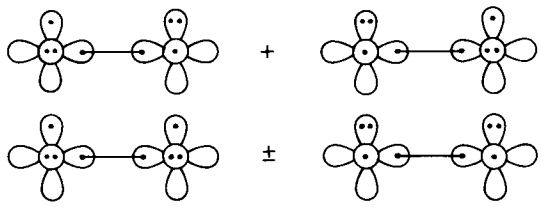

(49)

(50)

2. Chemisorption of O_2 to the (111) Si surface

Starting with the (111) surface of Si we find that the ground state of O_2 bonds so as to lead to a peroxy radical

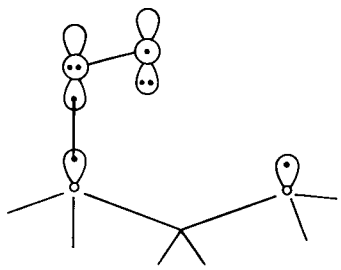

(51)

with an SiOO bond angle of 126°.[30] This state does not close directly to the bridged form

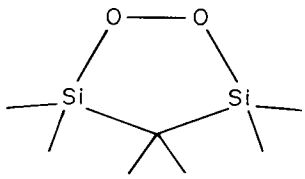

(52)

because the singly occupied orbital of the peroxy radical lies in the plane perpendicular to the SiOO plane. The terminal O has a doubly occupied lone pair orbital which interacts repulsively with the neighboring Si atom. The orbitals are shown in Fig. 7 and the energetics are sketched in Fig. 8. Bonding a ground state O_2 to the surface as a peroxy radical is exothermic by 2.3 eV, but the sticking coefficient is expected to be low[31] because (i) a part of the exothermicity in the SiO bond coordinate must be quickly converted into lattice vibrations, (ii) the bond requires specific orientation of the O_2 with respect to the surface, and (iii) there is probably a barrier (≥0.15 eV) in the potential curve for bonding O_2 to the surface.

There is an excited state of the surface peroxy radical that involves promotion of an electron between the nonbonding orbitals of the terminal O atom, much like the transition between configurations (49) and (50) of O_2 and with a similar excitation energy, 0.9 eV (as compared with 1.0 eV).[30] In this excited state, the terminal O atom may react with the surface by attacking an adjacent surface Si to form a bridged bond as in configuration (52) or (more likely) two chemisorbed O atoms as in (53)

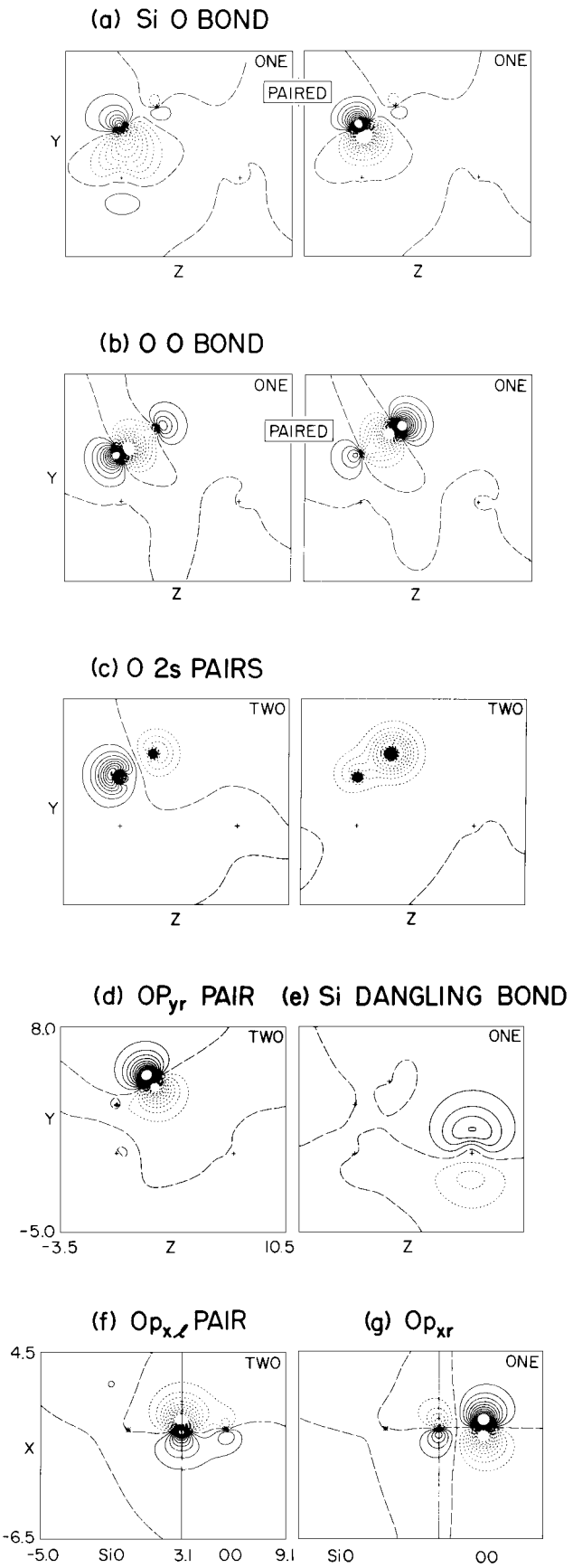

FIG. 7. The orbitals for chemisorbed molecular oxygen on Si (111). From calculations on the $Si_3H_6O_2$ complex. Conventions are the same as in Fig. 5 except that contour increments are 0.05 atomic units. The important orbitals here are (a) the SiO bond pair, (d) the oxygen lone pair orbital in the plane of the SiO bond, and (g) the radical orbital of the chemisorbed O_2 (in the plane perpendicular to the SiO_2 plane).

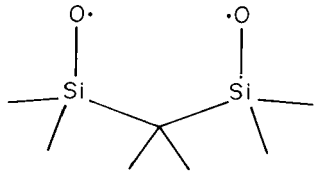

(53)

Alternatively, this excited state could also attack an Si–Si surface bond as in the following:

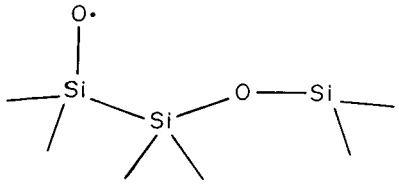

(54)

There are several important differences in the chemisorption of the excited singlet state of O_2 as compared with the ground state $^3O_2$. First, for $^1O_2$ the process of dissociative chemisorption (breaking the O–O bond and leaving one O atom on the surface with the other atom free to conserve energy and momentum conditions) is exothermic (by 0.5 eV). This does not require transfer of reaction exothermicity into lattice modes and hence the sticking coefficient should be greatly increased. Second, even assuming that the O_2 chemisorbs molecularly, the excited state peroxy radical species so formed [compare with configuration (50)] is more reactive (*vide supra*) and may further react before desorption. Third, there is probably no barrier in the potential curve for attack of $^1O_2$ on the surface. As a result, the sticking coefficient for $^1O_2$ on Si (111) is expected to be[31] much higher than for $^3O_2$.

Of course free oxygen atoms can also bond directly to the surface, leading to a radical of the form

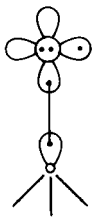

(55)

This bond is fairly ionic (charge transfer of ~1.0 electrons) and leads to a bond energy of 4.7 eV.[25] There is no energy barrier associated with bonding the O atom to the dangling

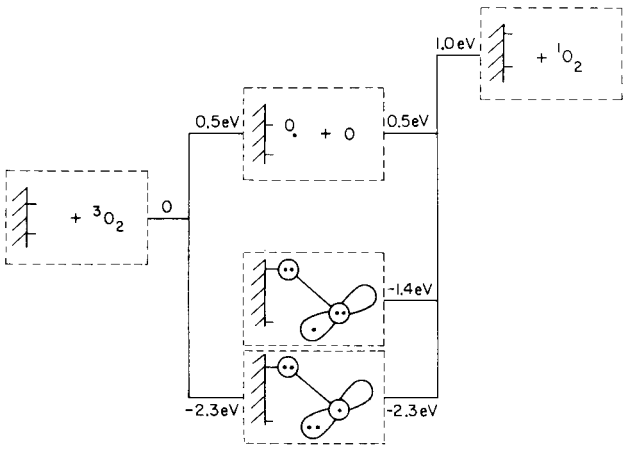

FIG. 8. Relative energies of $^3O_2$, $^1O_2$, and various species chemisorbed on Si.

bond orbital and there are no orientational restrictions of the type found for O_2. In addition, since there is a large charge transfer from Si to O and since the geometry of the surface Si changes markedly as the dangling bond electron is removed, there may be a much stronger coupling of the Si–O mode with the Si lattice modes, aiding energy transfer and thereby increasing the sticking coefficient. As a result of these various factors, the sticking coefficient for O atom on the surface is large ($S \sim 1$).[31]

It is possible that chemisorption of $^1O_2$ would lead to a particularly gentle oxidation of the surface. The bond energy of one O atom to the surface is 4.7 eV, whereas the O–O bond of the $^1O_2$ state is 4.2 eV. Thus it is 0.5 eV exothermic for one O to stick on the surface and for the other to carry off the excess energy in translation. As a result, no reaction exothermicity energy need be coupled into the phonon system and the sticking coefficient may be very large. With up to 0.5 eV of translational energy, the free O atom may escape the surface entirely (observation of these hot O atoms from the surface may provide a way of monitoring this dissociative chemisorption). The net result is little local heating. In contrast, chemisorption of $^3O_2$ or O atom puts 2.3 or 4.7 eV of exothermicity into local heating of the substrate, enough to disrupt or disorder the surface.

Some of the likely stages in the oxidation of Si surfaces are shown in Fig. 9. In step A the O–O bond is retained, leading to a peroxy radical, while in step B the O–O bond is broken but the O is still bonded only to a single surface atom. A later step C has the O atom bridging adjacent Si atoms (having broken an Si–Si bond) while ultimately (step E) the bonding is as in silica. Since O is much more electronegative than Si, there is a great deal of charge transfer ($\sim 1.0e$) in step B. In step A there is also a similar Si–O bond, but in this case the terminal oxygen has a lone pair in the plane that delocalizes back into the same SiO region (in the free molecule this lone pair is quite delocalized; localization decreases the O–O π bonding). The result of this competition between the Si orbital and the terminal O (both of which try to delocalize onto the first O) is that the charge transfer from the Si is much smaller ($\sim 0.6e$). In step C there is some additional charge transfer ($\sim 1.4e$) since there are two ionic bonds to the oxygen. However, the charge transferred from the Si ($\sim 0.7e$) is less than in step B. For step D the charge on each O should be about as in step C; however, the charge transferred from each Si should be twice as large ($\sim 1.4e$). This charge transfer will increase as the Si is further oxidized to the silica form (step E). Thus the sequence of A → B → C → D → E is one of increasing transfer of charge from the Si except for step (C).

Changes in the charges on the Si and O atoms should be indicated by chemical shifts in the XPS [particularly Si ($2p$) and O ($1s$)]. Spicer and co-workers[32] have searched for such effects by examining the chemical shift in the Si $2p$ level as a function of O_2 pressure and oxidation conditions. They find several phases formed sequentially upon exposure, leading to successively larger chemical shifts expected from the above analysis. This provides some experimental evidence for the theoretical models.

There is an interesting concentration dependence expected in these chemical shifts. For step A there is one affected Si per

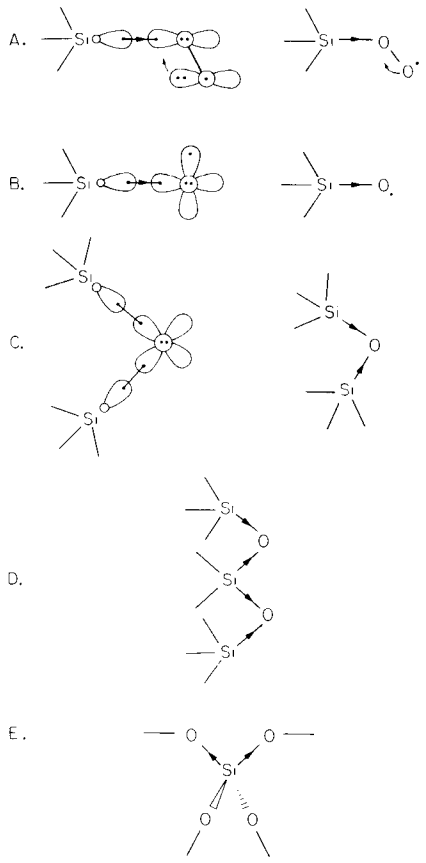

FIG. 9. Schematic diagram for various species chemisorbed on Si. Arrows are included to show the directions of charge transfer in ionic bonds.

every O_2 chemisorbed, whereas for step B there are two affected Si per every O_2. For shift C there are four affected Si per every O_2, whereas for shift D (as drawn) there is only strongly shifted Si and two less shifted ones. Ultimately for Si there are four affected Si per O_2. Additional evidence in favor of the peroxy radical (step A of Fig. 9) as the initial form of chemisorbed O_2 is provided by two experiments:

(i) Using XPS, Rowe *et al.*[33] have shown that the initial stage of O_2 chemisorption leads to two O $1s$ signals of comparable intensity but with different chemical shifts. This is, of course, just what is expected from the peroxy radical model.

(ii) Dorn *et al.*[34] have shown that the initial stage of O_2 chemisorption leads to three new vibrational modes with components perpendicular to the surface. This is just what is expected from the peroxy radical model.

IV. GaAs CALCULATIONS

A. Reconstruction

The unreconstructed (110) surface of GaAs is illustrated in Fig. 10(a). In modelling this surface we consider that a finite portion of the surface is sliced out of the solid and every Ga–As bond so cut is replaced by a bond to an H atom. In this way the proper hybridization is retained at each atom and there are no spurious radical centers. Thus the minimal complex for studying reconstruction of the GaAs surface is model 0 [see Fig. 10(b)] consisting of $Ga_1As_1H_4$, where the Ga and As are both surface atoms. A more complete complex is model 1 [see Fig. 10(c)] where the original Ga or As is bonded to three As

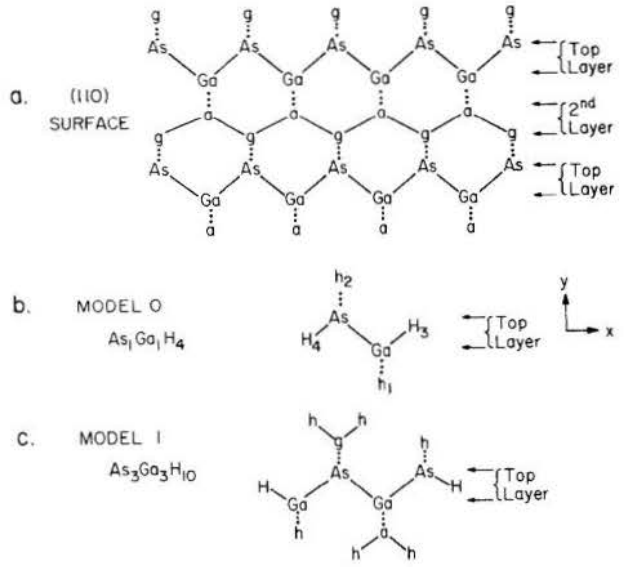

FIG. 10. The (110) surface of GaAs and model complexes.

or Ga neighbors, respectively. Here we will report only calculations with model 0.

The geometric variations were carried out as follows. (1) All second-layer atoms were fixed. (2) The surface Ga and the surface As were moved independently but with the constraint that the bond length to the (virtual) second-layer atoms be fixed and that there be no lateral displacements of this bond (that is, the surface atom remains in the yz plane defined by this AsGa interlayer bond and the normal to the surface). (3) The virtual surface atoms being represented by H atoms [H_3 and H_4 in Fig. 10(b)] are moved by the same amount as the real surface atoms of item (2).

With the above constraints there are two independent parameters remaining, one for the Ga and one for the As. These will be written as δz_{Ga} and δz_{As}, referring to the projection of the displacement upon the normal to the surface (positive δz is away from the surface); of course, $\delta z \neq 0$ implies $\delta y \neq 0$.

After one sequence of optimization, we obtained the results in Table I, with

$$\begin{aligned} \delta z_{As} &= +0.23 \text{ Å} \\ \delta z_{Ga} &= -0.47 \text{ Å}. \end{aligned} \tag{56}$$

Extensive experimental LEED studies combined with dynamic intensity calculations have been carried out by Mark, Duke, and co-workers,[35] obtaining the result that

$$\begin{aligned} \delta z_{As} &= +0.232 \text{ Å} \\ \delta z_{Ga} &= -0.468 \text{ Å}, \end{aligned} \tag{57}$$

TABLE I. Displacements (in Å) of the surface Ga and As of the reconstructed (110) surface of GaAs. [See Fig. 10(b).]

	δz_{As}	δz_{Ga}	δy_{As}	δy_{Ga}
Calculation	0.23	−0.47	0.41	0.50
Experimental[a]—Optimal	0.232	−0.468		
Experiment—34.8° twist[b]	0.208	−0.601	0.300	0.554

[a] Ref. 35.

[b] A constrained relaxation in which the GaAs bond length is kept fixed.

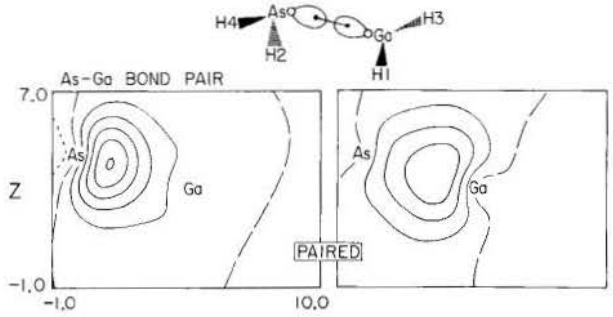

FIG. 11. The GaAs bond between surface atoms (reconstructed geometry) from GVB calculations on model 0. Conventions as in Fig. 7.

agreeing to within 0.01 Å with the theoretical value! This amazingly close agreement is in fact too close. Although our calculations use a good basis (valence double zeta plus d functions), we have not yet included electron correlation effects in the geometric optimization, and hence errors of up to 0.02 Å could have been expected. However, from the good description provided by the minimal complex, model 0, we may conclude here that the *surface reconstruction is determined by local rehybridization or valence effects* and is basically independent of band features.

The bond angles subtended at the As are 89°, 89°, and 107° for an average of 95°, close to the value of 93° found for free AsH_3. The bond angles at the Ga are 126°, 126°, and 107°, leading to an average of 120°, close to the value of 120° expected for free GaH_3. Thus the surface atoms come close to the expected valence angles.

Full generalized valence bond calculations were carried out at the optimum geometry, leading to the orbitals of the GaAs bond pair, as shown in Fig. 11. The left orbital is localized on the As (82% p character), while the right one is basically localized on the Ga (48% p character). Overall, the charge distribution of this bond pair leads to $0.82e$ on the Ga and $1.16e$ on the As (the balance is on other atoms) accounting for a transfer of 1/6 electrons from Ga to As. The two As lone pair orbitals (Fig. 12) are typical As lone pair orbitals with 33% p in character.

In Fig. 13 we show a plot of the potential surface for reconstruction of the surface. In order to reduce the figure to a one-dimensional curve, we have coupled the Ga and As distortions so that

$$\delta z_{As} = -1/2\delta z_{Ga}.$$

(Thus $\delta z = 0$ is the unreconstructed surface, while $\delta z = -0.47$

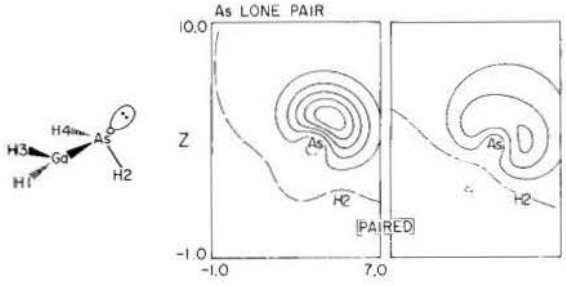

FIG. 12. The As lone pair for surface As (reconstructed geometry) from GVB calculations on model 0.

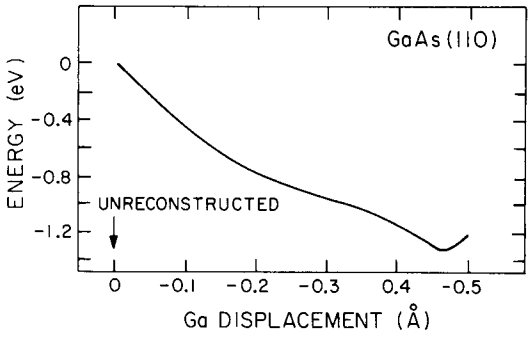

FIG. 13. The energy surface for reconstruction of GaAs. Here the motions of Ga and As are coupled so that $\delta z_{As} = -1/2\delta z_{Ga}$.

is close to the final minimum.) The total energy drop associated with the reconstruction is calculated to be 1.3 eV. This is in sharp contrast to the case of Si where the energy decrease upon relaxation of the surface Si was 0.024 eV (that is, about equal to kT for 300 K). Although the reconstruction energy is large compared with thermal energies, it is not large compared with chemical bond energies and indeed we find below that bonding O to either Ga or As tends to distort the surface toward the unreconstructed geometry (possibly a general effect of chemisorbed atoms).

B. Bonding of O atoms

As the first step in examining processes involved in oxidation of GaAs surfaces, we have examined the bonding of O atoms to simple GaH_3 and AsH_3 complexes.

We find that the O atom makes a strong bond to AsH_3. The As lone pair delocalizes toward the O, becoming a sigma bond, while the oxygen atom has two electrons in each of two O $p\pi$ orbitals,

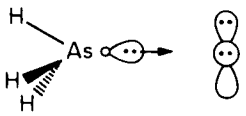

(58)

The bond energy is 4.0 eV with respect to AsH_3 plus $O(^1D)$, the corresponding state of O atom [the ground state $O(^3P)$ is 2.0 eV lower].

The HAsH bond angle of H_3AsO is 100.6° as compared with 93° for free AsH_3. Thus bonding of an O to the surface As is expected to push the As back toward the unreconstructed position. Concomitantly, the Ga would move back from planar toward a tetrahedral geometry. As a result of such coupling, the empty orbital on the Ga can be drastically modified by chemisorption of O, even though the O does not attack the Ga directly.

We find the bonding of O to GaH_3 to be quite different. Here the doubly occupied p orbital of the O is oriented toward the Ga, delocalizing somewhat into the empty Ga p orbital. The remaining two electrons are in singly occupied $p\pi$ orbitals on the O, leading to an overall triplet state,

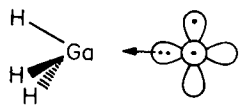

(59)

Although a relative minimum was found, the energy of this species is 1 eV above that of free H_3Ga plus O (^3P). The lesson here is that *for O atom to bond strongly to Ga one must break one of the three bonds to the Ga.* Spicer and co-workers have come to similar conclusions based on photoemission data.[36]

The optimum HGaH bond angle of H_3GaO was found to be 110.4°, as compares with 120° for the free GaH_3 species. Thus, as with As, bonding the O atom tends to distort the surface toward the unreconstructed configuration.

Important questions concerning oxidation of GaAs surfaces are: (1) What is the initial state of O_2 on the surface? (2) What is the chemical mechanism involved in decomposition of the O_2? (3) Where is the final location of the O? Many additional theoretical studies are required before such questions can be answered; however, the current work does provide some guidelines as follows: (a) O atom does make a strong bond to As without requiring disruption of the other three bonds to the As. (b) O atom does not make a strong bond to the Ga without disrupting one of the three bonds to the Ga. (c) Bonding O to As or Ga distorts the surface toward the unreconstructed positions.

A number of systems have been sutdied involving bonding of O_2 including the reaction of O_2 with O atom,[13] CH_2,[37] ethylene molecule,[38] hemoglobin,[39] and Si surface[30] (*vide supra*). In all cases the O_2 requires at least one singly occupied orbital to pair with in making a strong chemical bond. However, for GaAs at the reconstructed geometry there are no such orbitals to pair with the O_2 and even at the unreconstructed geometry there is not a real dangling bond orbital available. There is an empty orbital on the Ga but this does not bond strongly to the O lone pair orbital. As a result of these considerations, we conclude that molecular O_2 bonds only weakly (physical adsorption) to the perfect GaAs (110) surface. In our view, defect sites with a broken Ga–As bond are required to form a strong bond to molecular O_2. Indeed, such sites may catalyze the dissociation of O_2 into chemisorbed O atoms. These O atoms may then attack nearby Ga or As atoms even though O_2 would not. This O atom may then bond to As atoms of the perfect surface as in configuration (58) or may attack the AsGa bonds of the surface to form the oxide. Consequently, perfect (110) surfaces of GaAs should show a low sticking coefficient for $^3O_2$, a higher value for $^1O_2$, and even higher values for O atom. This is consistent with the observation by Mark and co-workers[40] that the sticking coefficient for oxygen on GaAs (110) surface is increased by orders of magnitude for the disordered surface over that for the ordered surface.

Spicer and co-workers[36] and Bauer[41] have concluded from photoemission studies that O_2 attacks the As site and that the Ga-derived empty state is modified. These results are consistent with the above picture since the final site for the O atom may be the As site even though the O_2 attacks a different site. Note that bonding the O to the As as in configuration (58) would also affect the geometry of the Ga (moving it toward the unreconstructed position). As a result, the empty orbital of the Ga is affected (changed from a nearly pure p orbital to tetrahedral and shifted down in energy) even though the O atom has attacked the As.

We see that (110) GaAs is quite different from (111) Si in essential respects. For (111) Si there are radical orbitals on the

Si ready to pair up with radical orbitals on the O or O_2 to form strong covalent bonds as in configurations (49) and (53). Thus it is quite reasonable that molecular O_2 chemisorbs as in configuration (49). However, for (110) GaAs the orbitals of the perfect surface are strongly paired with no radical centers for making a bond to molecular O_2 as in (49). Consequently we do *not* expect *molecular* O_2 to bond strongly to the perfect (110) GaAs surface.[42]

V. CONCLUSIONS

It should be clear from the above discussions that we have barely scratched the surface on the applications of *ab initio* quantum chemical technqiues to problems involving the solid–gas interface. Even so, we believe that the insights obtained from these initial studies indicate that the chemical approach will be quite valuable in elucidating surface phenomena. The major advantages of this chemical approach are

(i) electron correlation (many-body) effects are included explicitly (and self-consistently) so that the energetics of bond formation and bond disruption processes should be reliable;

(ii) total energies are obtained directly, allowing detailed consideration of the geometries and energetics of reconstruction, chemisorption, and oxidation.

(iii) the orbital picture abstracted directly from the calculations provides a conceptual framework useful in understanding the theoretical and experimental results and in extrapolating these results to new systems.

Such studies should lead to detailed mechanisms for the chemical processes on surfaces. We would hope that the general principles extracted from such studies will be useful in developing experimental techniques aimed at providing specific surface properties.

There are, however, flaws that must be overcome for the chemical approach to be of general applicability in surface problems. A major problem is that even a qualitatively correct description of the band structure of the solid requires 50 to 100 atoms and a convincing analysis of such surface structures as Si (111) 7×7 requires at least ~50 *surface* atoms. Thus techniques must be found for efficient application of *ab initio* correlated wavefunctions to very large clusters. Probably the ultimate method will involve a correlated wavefunction for surface states self-consistently matched on to a more traditional treatment of the band states.

Even so, the work described herein indicates that qualitatively useful, semiquantitative data about the gas–surface interface can be obtained by proper treatment of very small molecular complexes.

ACKNOWLEDGMENTS

The authors gratefully acknowledge useful discussions with Professors W. E. Spicer, P. Mark, and R. S. Bauer. One of us (TCM) would like to acknowledge the support of the Alfred P. Sloan Foundation. This work (Contribution No. 5770) was supported in part by a grant from the Director's Discretionary Fund of the Jet Propulsion Laboratory and by a grant from the National Science Foundation (DMR74-04965).

[1]See, for example, J. A. Appelbaum and D. R. Hamman, Rev. Mod. Phys. **48,** 479 (1976) and references cited therein.

[2]A detailed discussion and review of SCF methods is contained in F. W. Bobrowicz and W. A. Goddard III, *Modern Theoretical Chemistry: Methods of Electronic Structure Theory,* edited by H. F. Schaefer III (Plenum, New York, 1977), Vol. 3, pp. 79–127.

[3]In equations such as (1), (18), (20), (21), and (22), electron numbers will be suppressed with the understanding that a product of functions is always in the sequence of increasing electron number. Thus $\phi_a\phi_b\phi_c \cdot = \phi_a(1)\cdot\phi_b(2)\phi_c(3)$.

[4]J. C. Slater, in *The Self-Consistent Field for Molecules and Solids* (McGraw-Hill, New York, 1974).

[5]K. H. Johnson and F. C. Smith, Jr., Phys. Rev. B **5,** 831 (1972).

[6]See, for example, E. J. Mele and J. D. Jounnopoulos, Phys. Rev. B **17,** 1816 (1978); D. J. Chadi, Phys. Rev. B (in press).

[7]R. Hoffmann, J. Chem. Phys. **39,** 1397 (1963).

[8]J. C. Phillips and L. Kleinman, Phys. Rev. **116,** 287 (1959); H. Hellmann, J. Chem. Phys. **3,** 61 (1935).

[9]U. Mitzdorf, Theor. Chim. Acta **37,** 129 (1975).

[10]J. W. D. Connolly and J. R. Sabin, J. Chem. Phys. **56,** 5529 (1972); C. H. Li and J. W. D. Connolly, Surf. Sci. **65,** 700 (1977).

[11]W. A. Goddard III and R. C. Ladner, J. Am. Chem. Soc. **93,** 6750 (1971); W. A. Goddard III and L. B. Harding, Ann. Rev. Phys. Chem. **29,** 000 (1978) (in press).

[12]W. A. Goddard III, T. H. Dunning, Jr., W. J. Hunt, and P. J. Hay, Acc. Chem. Res. **6,** 368 (1973).

[13]P. J. Hay, T. H. Dunning, Jr., and W. A. Goddard III, Chem. Phys. Lett. **23,** 457 (1973); J. Chem. Phys. **62,** 3912 (1975).

[14]L. B. Harding and W. A. Goddard III, J. Chem. Phys. **67,** 1777, 2377 (1977); S. P. Walch and W. A. Goddard III, J. Am. Chem. Soc. **100,** 1338 (1978).

[15]W. A. Harrison, *Pseudopotentials in the Theory of Metals* (Benjamin, New York, 1966).

[16]C. F. Melius and W. A. Goddard III, Phys. Rev. A **10,** 1528 (1974); see also W. A. Goddard III, Phys. Rev. **174,** 659 (1968); L. R. Kahn and W. A. Goddard III, J. Chem. Phys. **56,** 2685 (1972); C. F. Melius, B. D. Olafson, and W. A. Goddard III, Chem. Phys. Lett. **28,** 457 (1974); A. Redondo, W. A. Goddard III, and T. C. Mcgill, Phys. Rev. B **15,** 5038 (1977).

[17]See, for example, J. R. Chelikowsky and M. L. Cohen, Phys. Rev. B **14,** 556 (1976); Phys. Rev. B **13,** 826 (1976).

[18]J. A. Appelbaum and D. R. Hamann, Phys. Rev. Lett. **31,** 106 (1973); Phys. Rev. Lett. **32,** 225 (1974).

[19]See, for example, D. Haneman, J. Vac. Sci. Technol. **15,** 1267 (1978).

[20]See, for example, J. A. Appelbaum and D. R. Hamann, Phys. Rev. Lett. **34,** 806 (1975).

[21]J. Goodisman, *Diatomic Interaction Potential Theory* (Academic, New York, 1973), Vol. I.

[22]J. A. Appelbaum, D. R. Hamann, and K. H. Tasso, Phys. Rev. Lett. **39,** 1487 (1977).

[23]A. K. Rappé, T. A. Smedley, J. J. Barton, M. L. Steigerwald, M. M. Goodgame, R. A. Bair, and W. A. Goddard III (to be published). See also T. A. Smedley, Master's Thesis, (California Institute of Technology, 1978).

[24]A. Redondo, W. A. Goddard III, T. C. McGill, and G. T. Surratt, Solid State Commun. **20,** 733 (1976).

[25]A. Redondo, Ph.D. Thesis (California Institute of Technology, 1976).

[26]J. E. Rowe, M. M. Traum, and N. V. Smith, Phys. Rev. Lett, **33,** 1333 (1974).

[27]H. D. Shih, F. Jona, D. W. Jepson, and P. M. Marcus, Phys. Rev. Lett. **37,** 206 (1976).

[28]P. Mark, J. D. Levine, and S. H. McFarlane, Phys. Rev. Lett. **38,** 1408 (1977).

[29]B. J. Moss and W. A. Goddard III, J. Chem. Phys. **63,** 3523 (1975).

[30]W. A. Goddard III, A. Redondo, and T. C. McGill, Solid State Commun. **18,** 981 (1976).

[31]There is a great deal of uncertainty concerning sticking coefficients (S) of O_2 on Si. R. J. Madix and A. A. Susu [Surf. Sci. **20,** 377 (1970)] showed that $S = 0.3$ to 0.6 for O atoms. R. Dorn, H. Lüth, and H. Ibach [Surf. Sci. **42,** 583 (1974)] showed that $S \approx 10^{-3}$ if the ion gauge is on and nude while S is a factor of 10 smaller if the gauge is on but enclosed. Spicer *et al.* (Ref. 36) showed for O_2 on GaAs that even when enclosed, having the ion gauge

on leads to a higher S than when the gauge is off. Based on these results, the best experimental estimate for $^3O_2$ is $S \leq 10^{-4}$. The effect of the ion gauge is probably due to either (a) dissociation of O_2 to form a small concentration ($\sim 10^{-3}$) of O atoms or (b) excitation of a part (say $\sim 1\%$) of the O_2 to the $^1O_2$ state coupled with a higher S for $^1O_2$ than for $^3O_2$ (say $S \approx 10^{-2}$).

[32]C. M. Garner, I. Lindau, C. Y. Su, P. Pianetta, J. N. Miller, and W. E. Spicer, Phys. Rev. Lett. **40,** 403 (1978).

[33]J. E. Rowe, G. Margaritondo, H. Ibach, and H. Froitzhein, Solid State Commun. **20,** 277 (1976).

[34]R. Dorn, H. Lüth, and H. Ibach, Surf. Sci. **42,** 433 (1974).

[35]P. Mark, G. Cisneros, M. Kahn, C. B. Duke, A. Paton, and A. R. Lubinsky, J. Vac. Sci. Technol. **14,** 910 (1977).

[36]P. Pianetta, I. Lindau, C. M. Garner, and W. E. Spicer, Phys. Rev. Lett. **37,** 1166 (1976); Phys. Rev. Lett. 35, 1356 (1975); P. W. Chye, P. Pianetta, I. Lindau, and W. E. Spicer, J. Vac. Sci. Tech nol. **14,** 917 (1977); W. E. Spicer, P. Pianetta, I. Lindau, and P. W. Chye, J. Vac. Sci. Technol. **14,** 885 (1977).

[37]W. R. Wadt and W. A. Goddard III, J. Am. Chem. Soc. **97,** 3004 (1975).

[38]L. B. Harding and W. A. Goddard III, J. Am. Chem. Soc. **99,** 4250 (1977); Tetrahedron Lett. 747 (1978).

[39]B. D. Olafson and W. A. Goddard III, Proc. Natl. Acad. Sci. USA **74,** 1315 (1977).

[40]P. Mark, S. C. Chang, W. F. Creighton, and B. W. Lee, CRC Crit. Rev. Solid State Sci. **5,** 189 (1975); P. Mark, E. So, and M. Bonn, J. Vac. Sci. Technol. **14,** 865 (1977).

[41]R. S. Bauer, J. Vac. Sci. Technol. **14,** 899 (1977).

[42]This conclusion is apparently in disagreement with the assumption in recent studies by E. J. Mele and J. D. Joannopoulos [Phys. Rev. Lett. **40,** 341 (1978)]. They carried out tight-binding calculations assuming that for the perfect GaAs surface the O_2 is bonded to the As as a peroxy radical [as in Si (Ref. 30)] and found agreement with the experimental photoemission. However, it is quite possible that similar results would be obtained for tight-binding calculations using O chemisorbed to As as in configuration (58).